Diaphragm shear modulus reflects transdiaphragmatic pressure Diaphragm shear modulus reflects transdiaphragmatic pressure 1 during isovolumetric inspiratory efforts and ventilation against inspiratory loading

Damien Bachasson, Martin Dres, Marie-Cecile Nierat, Jean-Luc Gennisson, Jean-Yves Hogrel, Jonne Doorduin, Thomas Similowski

Diaphragm shear modulus reflects transdiaphragmatic pressure during isovolumetric inspiratory efforts and ventilation against inspiratory loading

Damien Bachasson*[#1], ***Martin Dres***[#2,3], ***Marie-Cécile Niérat***[3], ***Jean-Luc Gennisson***[4], ***Jean-Yves Hogrel***[1], ***Jonne Doorduin***[5], ***Thomas Similowski***[2,3]

[1]Institute of Myology, Neuromuscular Investigation Center, Neuromuscular Physiology Laboratory, Paris, France

[2]AP-HP, Groupe Hospitalier Pitié-Salpêtrière Charles Foix, Service de Pneumologie, Médecine Intensive et Réanimation, (*Département "R3S"*), F-75013, Paris, France

[3]Sorbonne Université, INSERM, UMRS1158 Neurophysiologie respiratoire expérimentale et clinique, F-75005 Paris, France

[4]Imagerie par Résonance Magnétique Médicale et Multi-Modalités (IR4M), CNRS UMR8081, Université Paris-Saclay, Orsay, France

[5]Department of Neurology, Donders Institute for Brain, Cognition and Behaviour, Radboud University Medical Center, Nijmegen, The Netherlands

[#]Both authors equally contributed to this work.

*Address for correspondence: Institute of Myology, Neuromuscular Investigation Center, Neuromuscular Physiology Laboratory, Hôpital Universitaire Pitié Salpêtrière, Paris 75651 Cedex 13, France. Tel: +33 1 42 16 66 41; fax: +33 1 42 16 58 81. E-mail address: d.bachasson@institut-myologie.org

Abstract

Aim. The reference method for the assessment of diaphragm function relies on the measurement of transdiaphragmatic pressure (Pdi). Local muscle stiffness measured using ultrafast shear wave elastography (SWE) provides reliable estimates of muscle force in locomotor muscles. This study aimed at investigating whether SWE could be used as a surrogate of Pdi to evaluate diaphragm function.

Methods. Fifteen healthy volunteers underwent a randomized step-wise inspiratory loading protocol of 0-60% of maximal isovolumetric inspiratory pressure during closed-airways maneuvers and 0-50% during ventilation against an external inspiratory threshold load. During all tasks, Pdi was measured and SWE was used to assess shear modulus of the right hemi-diaphragm (SMdi) at the zone of apposition. Pearson correlation coefficients (r) and repeated measures correlation coefficient (R) were computed to determine within individual and overall relationships between Pdi and SMdi, respectively.

Results. During closed-airways maneuvers, mean Pdi correlated to mean SMdi in all participants (r ranged from 0.77 to 0.96, all $p < 0.01$; $R = 0.82$, 95% CIs [0.76, 0.86], $p < 0.01$). During ventilation against inspiratory threshold loading, Pdi swing correlated to maximal SMdi in all participants (r ranged from 0.40 to 0.90, all $p < 0.01$; $R = 0.70$, 95% CIs [0.66, 0.73], $p < 0.001$). Changes in diaphragm stiffness as assessed by SWE reflect changes in transdiaphragmatic pressure.

Conclusion. SWE provides a new opportunity for direct and non-invasive assessment of diaphragm function.

New & Noteworthy

Accurate and specific estimation of diaphragm effort is critical for evaluating and monitoring diaphragm dysfunction. The measurement of transdiaphragmatic pressure requires the use of invasive gastric and esophageal probes. In the present work, we demonstrate that changes in diaphragm stiffness assessed with ultrasound shear wave elastography reflect changes in transdiaphragmatic pressure, therefore offering a new noninvasive method for gauging diaphragm effort.

Introduction

The evaluation and monitoring of respiratory muscle function in general and of diaphragm function in particular are clinically relevant in a variety of clinical settings, among which weaning from mechanical ventilation (20). Routine measurements of respiratory function like those of volumes, flows, and gas exchange, are nonspecific and only give indirect information about respiratory muscle function. A more specific approach to quantitatively asses respiratory muscle function relies on the measurement of their force producing capacity (1). Yet there is currently no method directly giving access to respiratory muscle force in humans, hence the reliance on pressure differences to assess respiratory muscle function. Likewise, the reference method for the assessment of diaphragm function is the measurement of the transdiaphragmatic pressure (Pdi). Pdi is defined as the difference between pleural and abdominal pressures that are inferred from esophageal pressure (Pes) and gastric pressure (Pga), respectively (1). As the diaphragm is the only muscle that simultaneously lowers Pes and increases Pga, Pdi is considered as the most specific approach to assess diaphragm function. Pdi is not a direct reflection of diaphragm strength insofar as it depends on an array of factors governing the transformation of force into pressure (such as lung volume as a determinant of diaphragm length, thoracic and abdominal compliances, and thoracoabdominal configuration that can critically affect Pdi irrespective of any change in diaphragm strength (5).Yet Pdi is clinically relevant in that it represents the actual force that drives lung volume changes and therefore, ultimately, alveolar ventilation. Of note, measuring Pdi requires the use of esophageal and gastric probes, which impedes its generalization as a clinical tool.

Diaphragm ultrasound imaging allows the noninvasive measurement of diaphragm excursion, thickness and thickening (26, 31). Diaphragm thickening fraction has been shown to be an efficient tool for identifying diaphragm dysfunction, monitoring its temporal changes, and predicting weaning outcomes in ventilated patients (10, 11). However, equivocal relationships between Pdi and diaphragm thickening fraction have been reported (12, 23, 29),. Ultrasound shear wave elastography (SWE) is a recently available imaging method

allowing direct and real-time quantification of tissue mechanical properties (16). Briefly, SWE relies on the measurement of propagation velocity of shear waves remotely generated inside tissues by ultrasonic focused beams. Shear modulus can be readily estimated from the measured shear wave propagation velocity and tissue density (4). Local muscle stiffness measured using SWE has been shown to provide reliable estimates of muscle force in locomotor muscles (15, 18). Recently, Chino et al. (7) reported that the shear modulus of the diaphragm (SMdi) increases along with mouth pressure (Pmo) during isovolumetric inspiratory efforts. However, the relationship between SMdi and Pdi remains to be investigated.

Therefore, the aim of this study was to investigate the potential of ultrasound shear wave elastography to evaluate diaphragm function in healthy subjects during isovolumetric inspiratory efforts and during ventilation against inspiratory loads. We hypothesized that changes in SMdi would reflect changes in Pdi.

Materials and Methods

Participants

All participants gave written informed consent. This study conformed to the Declaration of Helsinki and was approved by the local ethics committee (Comité de Protection des Personnes iIe-de-France VI, France). The study was publicly registered prior to the first inclusion (ClinicalTrials.gov, NCT03313141).

Experimental setup

Participants were studied in a semirecumbent position (40 degrees) with uncast abdomen, breathing through a mouthpiece while wearing a nose clip. The mouthpiece was connected to a two-way valve and pneumotachograph (3700 series, linearity range 0–160 L*min-1; Hans Rudolph, Kansas City, MO) for flow measurement. Pmo was recorded using a differential transducer (model DP45–18, Validyne, Northridge, CA). Pes and Pga were measured using 8-cm balloon catheters (C76080U; Marquat Génie Biomédical, Paris,

France), connected separately to differential pressure transducers (model DP45-32; Validyne, Northridge, CA) as previously described (30). Flow and pressures signals were digitized (Powerlab, ADInstruments, Sydney, Australia) and recorded at a sampling frequency of 2 kHz (Labchart, ADInstruments). Pdi was obtained by online subtraction of Pes from Pga.

Ultrasound measurements. Diaphragm ultrasound imaging and shear wave elastography were performed using an Aixplorer Ultrasound scanner (V11.2, Supersonic Imagine, Aix-en-Provence, France) driving a 10-2 MHz linear transducer array (SL10-2, Supersonic Imagine). Settings were defined as follow: B-mode enabled; supersonic shear wave imaging mode enabled (SWE); penetration mode enabled; tissue tuner at 1540 $m \cdot s^{-1}$; dynamic range at 80 *dB*. Gain and time gain compensation were tailored for each patient. Sampling rates for B-mode imaging and SWE were 12 and 2 Hz, respectively. A generous amount of ultrasound gel was used during scanning for optimal acoustic coupling and minimal pressure was applied to the transducer in order to limit tissue deformation and modification of ventilatory mechanism. The right hemi-diaphragm was scanned at the zone of apposition, on the posterior axillary line vertical to the chest wall at the 8^{th}-10^{th} intercostal space. The right hemi-diaphragm was identified as a three-layered structure comprising two hyperechoic lines representing the pleural and peritoneal membranes and a middle hypoechoic layer representing the diaphragmatic muscle fibers. The rotation and angle of the transducer was then finely adjusted to obtain maximal echo intensity from diaphragmatic pleura and peritoneal membrane. The location of the probe was carefully marked on the skin to ensure reliable positioning of the probe within the protocol. Ultrasound acquisition were triggered with the Powerlab for synchronizing ultrasound, flow, and pressures recordings. Ultrasound measurements were performed by a trained operator (MD). An overview of the setup and samples of diaphragm ultrasound imaging is provided in Figure 1.

Study protocol

The study was carried out as follows: i) measurement of maximal isovolumetric inspiratory pressure (PImax), ii) recordings during apnea at functional residual capacity (FRC), iii) recordings during inspiratory efforts against closed airways, iv) recordings during ventilation against inspiratory threshold loading. Each step of the protocol was performed twice.

Maximal isovolumetric inspiratory pressure. PImax was measured at FRC. At least five trials were performed until three reproducible efforts, with less than 10% variance, were obtained (1). Maximal Pmo generated amongst the three reproducible trials was defined as PImax.

Apnea at FRC and isovolumetric inspiratory efforts against closed airways. During these tasks, the mouthpiece was disconnected from the three-way valve and flow was not monitored. Pressures and SMdi were measured during ~5s open glottis apnea and during inspiratory efforts against closed airways at 10, 20, 30, 40, 50, and 60 % of PImax. Both apnea and inspiratory efforts were performed at FRC. Participants were asked to reach progressively the target Pmo and to maintain their effort during ~10s. Visual feedback of generated Pmo and guidelines were provided to participants using the built-in software option. Each task was repeated twice. Tasks were alternated with 1-2 min of unloaded breathing.

Ventilation against inspiratory threshold loading. An in-house developed apparatus (23) modified from Chen et al. (6) was used to perform ventilation against inspiratory threshold loads. Briefly, the device consisted of a cylindrical adjustable pressure chamber connected to a non-rebreathing valve. The negative pressure was generated by a commercially available vacuum cleaner. Pressure in the chamber (Pch) was measured continuously using a differential pressure transducer (model DP45-32; Validyne, Northridge, CA). The dead space of the device was estimated at ~600 ml. Participants underwent a step-wise inspiratory threshold loading protocol at 10, 20, 30, 40 and 50% of PImax. Each task was repeated twice. During each task, at least six regular respiratory cycles were recorded. Tasks were alternated with 1-2 min of unloaded breathing.

Data analysis

Pes, Pga, Pdi, Pmo, Pch and flow were analyzed offline using standardized scripts in MATLAB (Mathworks, Natick, MA, USA). Frames from B-mode and SWE recordings were exported using the ultrasound scanner research pack (Soniclab, v12, Supersonic imagine) and each clips were processed offline using standardized scripts in MATLAB (Mathworks). A square region of interest (ROI) was drawn within the shear modulus map (see Figure 1) of the first frame of each clip between the diaphragmatic pleura and peritoneal. The latter ROI was replicated on other frames. SMdi was calculated assuming a linear elastic behavior in muscle tissue (4) as SMdi = $\rho \cdot V_s^2$ where ρ is the density of muscle (1000 kg·m^{-3}), and Vs is the shear wave speed in m·s^{-1}. Values with each ROI were averaged and reported as SMdi. For measurements during isovolumetric inspiratory efforts, signals were manually selected when Pmo was stabilized at the targeted levels. Pressures and SMdi where then averaged over the duration of the selected period. During ventilation against inspiratory threshold loading, maximal SMdi and pressures variations (*i.e.* Pmo, Pes, Pga, Pdi) within inspiratory time were computed for each cycle. Cycles were discarded if diaphragm visualization was lost during the acquisition, or in the presence of lung artefacts. Mean SMdi at functional residual capacity during apnea was subtracted from mean SMdi or maximal SMdi (within inspiratory time) during isovolumetric efforts and ventilation, respectively.

Statistics

Data within text and tables are presented as mean ± SD and mean [95% CIs] for correlation coefficients. The assumptions of normality and sphericity were confirmed using the D'Agostino's K-squared and Mauchly's tests, respectively. Repeated measures ANOVAs were conducted to evaluate change in variables depending on conditions. Tukey's HSD post-hoc tests were conducted when significant effect was found. Pearson correlation coefficients (r) were used for determining within-individual relationships between variables. For isovolumetric efforts, coefficients of variation were computed to assess the variability of Pdi and SMdi within the selected periods. Repeated measures correlation coefficient (R) were used for determining overall relationships between

variables (3). This statistical technique is used for determining the common within-individual association for paired measures assessed on two or more occasions for multiple individuals. This allows removing biases caused by violation of independence and/or differing patterns between-participants *versus* within-participants when performing simple correlation on aggregated data. All analyses were performed in the computing environment R version 3.2.4 (28). Statistical significance was set at $p < 0.05$ for all tests.

Results

Fifteen healthy participants (11 men, age = 32 years (min-max, 18-43), BMI = 24 $kg \cdot m^{-2}$ (SD 2.6); 4 women, age = 28 years (min-max, 20-44), BMI = 21.3 $kg \cdot m^{-2}$ (SD 1.3)) were studied. Mean PImax was 120 cmH_2O (SD 26) and mean SMdi during apnea at FRC was 9.13 kPa (SD 2.17). Body weight and PImax were significantly correlated ($r = 0.76$, $p < 0.01$.).

Isovolumetric inspiratory effort against closed airways. Typical recordings from isovolumetric submaximal inspiratory efforts are shown in Figure 2 (see also Supplemental Video S1 [https://figshare.com/s/eb987ad33ec4218e2cae]). Two participants did not perform isovolumetric inspiratory efforts against closed airways and two participants did not performed 60% PImax. Ultimately, the 89 available acquisitions were used for analysis. Mean selection duration for averaging data was 8.7 s (SD 3.9). Within selected data, mean of coefficient of variation for Pmo, Pes, Pga, Pdi, and SMdi were 14.2, 9.0, 6.3, 5.4, and 16.2 %, respectively. Pressures, and SMdi for all levels of inspiratory effort are displayed in Table 1 and Figure 3A. Repeated measures ANOVA showed significant effect of inspiratory effort levels on SMdi and Pdi. Relationship between mean Pdi swing and mean SMdi during all tasks for all data points is displayed in Figure 3B. Mean Pdi significantly correlated to mean SMdi in all participants (r ranged from 0.77 to 0.96, all $p < 0.01$; $R = 0.82$, 95% CIs [0.76, 0.86]). Individual correlation coefficients and individual datapoints are shown in Table 2 and Figure 4, respectively.

Ventilation against inspiratory threshold loading. Typical recordings from ventilation against inspiratory threshold loading in Figure 5 (see also Supplemental Video S2 [https://figshare.com/s/28abd0263f7df2285b65]). Two participants (5, 10) did not performed 50% PImax, one participant did not performed 40% PImax, and one participant additionally performed 60% PImax). Ultimately, 66 cycles were discarded over 970-recorded cycles because of aberrant SMdi values caused by loss of diaphragm visualization or lung artefacts during the acquisition. The number of cycles analyzed per loading level was 11.8 (SD 3.0). Flow, Pressures, and SMdi for unloaded breathing and all levels of inspiratory levels are displayed in Table 3 and Figure 6A. Repeated measures ANOVA showed significant effect of inspiratory threshold loading levels on SMdi and Pdi. Relationship between Pdi swing and maximal SMdi for all analyzed cycles and all loading tasks is displayed in Figure 6B. Maximal SMdi correlated to Pdi swing in all participants (r ranged from 0.40 to 0.90, all $p < 0.01$; $R = 0.70$, 95% CIs [0.66, 0.73], $p < 0.001$). Individual correlation coefficients and individual datapoints are shown in Table 4 and Figure 7, respectively.

Discussion

The aim of the present study was to investigate the potential of ultrasound shear wave elastography for evaluating diaphragm function in healthy subjects. We found that shear wave modulus of the diaphragm (*i.e.* stiffness) was strongly correlated with transdiaphragmatic pressure during both isovolumetric inspiratory efforts and inspiratory threshold loading.

As expected, increasing the inspiratory load during both isovolumetric inspiratory efforts and ventilation against inspiratory threshold loading resulted in an increase in Pdi (Table 1 and Figure 3; Table 3 and Figure 6, respectively). It should be noted that during unloaded breathing, Pdi and tidal volume were larger than expected for healthy subjects (Table 3) (9). This is most likely the result of the additional resistance and instrumental dead space imposed by the experimental device. Accordingly, variations in Pmo expressed as a percentage of

PImax were greater than pressure within the inspiratory loading device. Our data showed strong linear relationship between mean SMdi and Pdi during submaximal isovolumetric inspiratory efforts (Figure 3). These findings demonstrate that diaphragm stiffening is strongly related to the level of diaphragm activation as assessed by Pdi measurements. These findings are in line with the repeatedly demonstrated linear relationship between muscle shear modulus and active muscle force in locomotor muscles (2, 15, 18, 21). These results are also in agreement with the recent work by Chino et al. (7) that reported significant correlation between SMdi and Pmo during similar isovolumetric inspiratory efforts at FRC. However, we reported lower SMdi values for given isovolumetric inspiratory efforts *e.g.* mean SMdi was 63 kPa (SD 16) at 50% of PImax *versus* 29 kPa (SD 13) in the present work. Diaphragm recruitment is known to be reduced during voluntary inspiratory efforts in the semirecumbent position compared to the sitting position that was used in the study by Chino et al. (19). A lower ability of the participants to efficiently recruit their diaphragm may also contributed to explain these results. Our data also show strong linear relationship between max SMdi and Pdi swing during ventilation against inspiratory threshold loading. These findings demonstrate for the first time that diaphragm function can be noninvasively monitored using SWE during breathing. Besides one report in the cardiac muscle (8), this is also the first report supporting that SWE may be used to monitor dynamic muscle contractions. Although we found high individual correlation coefficients between SMdi and Pdi in most participants, our data showed that SMdi may fail to increase along with Pdi during both isovolumetric inspiratory efforts (*i.e.* participants 5, 11, 12; Figure 4 and Table 2) and during ventilation against inspiratory threshold loading (*i.e.* participants 5, 12, 15; Figure 7 and Table 4). These findings may be explained, at least in part, by misalignment of the transducer according to the direction of diaphragm fascicles. This factor has been repeatedly identified as critical given the highly anisotropic nature of the skeletal muscle (17). Slight offset of transducer angle in reference to the direction of muscle fascicles reduces shear modulus value (17). Therefore, quality criteria for SMdi measurements must be established and adjustment of transducers in the three-dimensional space shall be assisted programmatically to obtain largest SMdi changes during ventilation. Another potential explanation is

222 that Pdi is an indirect reflect of diaphragm force, insofar as the its generation is influenced by factors such as
223 lung volume, thoracoabdominal compliances and thoracoabdominal geometrical configuration (see
224 introduction). Also, Pdi can be contributed to by extra diaphragmatic inspiratory muscles or by expiratory
225 muscles if the transmission of the pressure that these muscle generate across the diaphragm is incomplete,
226 which can occur in the presence of concomitant contraction of the diaphragm with other respiratory muscles
227 (14, 27). Thus, high Pdi values can be reached in certain circumstances with limited contribution of the
228 diaphragm. Interestingly, we observed less steep relationship between SMdi and Pdi during isovolumetric effort
229 as compared to ventilation against threshold inspiratory loading. This may be explained, at least in part, by the
230 fact that efforts were performed at functional residual capacity during submaximal isovolumetric effort *i.e.*
231 closer to diaphragm optimal length as compared to ventilation against threshold inspiratory loading where peak
232 Pdi is reached at higher pulmonary volume.

233 *Limitations.* Participants were free to use any strategy to reach the target during isovolumetric inspiratory effort
234 (with a Pmo rather that a Pdi target) or to overcome inspiratory loads during ventilation tasks. This may have
235 led to poor diaphragm recruitment. Within the present study, SWE frame rate was limited to 2 Hz and this may
236 contribute, at least in part, to reduce the amplitude of SMdi variations. Increase in SWE frame rate represents a
237 critical challenge to fully exploit the potential of SMdi measurements. Oppersma et al. (23) recently
238 demonstrated that diaphragm strain and strain rate assessed using speckle tracking outperform conventional
239 ultrasound methods. Comparison of SMdi with strain-derived metrics and conventional thickening fraction
240 remain to be investigated. Ultrasound muscle imaging is highly operator dependent. Change in transducer
241 position might have occurred, in particularly with large thorax movement and this may contribute to explain
242 inferior SWE performance in some participants. As previously observed during pretests, SMdi could not be
243 assessed during maximal inspiratory maneuvers. It is unlikely that diaphragm SWE may be accurately used as
244 performed within this study during maximal inspiratory maneuvers because of sudden thorax movement and
245 large diaphragm deformation. Collectively, these findings emphasize the need to develop specifically designed

skin-transducer interfaces and optimized post processing methods for reducing these confounding effects. In addition, both intra- and inter-operator reliability of SMdi measurements remain to be evaluated. The limited frame rate of SWE mentioned above also prevent the use of SWE during electrical/magnetic phrenic nerve stimulation or brief volitional maneuvers such as the sniff test (1). Although SWE frame rate may be substantially increased (8), it will most likely remain too low for capturing such short events because shear waves must first travel through the tissue to be filmed (16). Similarly to conventional ultrasound methods, lung sliding may block a good view on the diaphragm when tidal volume increases (26). This may therefore prevent us from using diaphragm SWE when ventilatory demand is increased *e.g.* during exercise and/or with higher inspiratory volume. This will be investigated in future works. At last, increase diaphragm depth caused by thicker subcutaneous tissue in overweighed patients may also affect SMdi measurements (13).

Perspective and clinical implications. Diaphragm SWE appears to have a strong potential for direct, noninvasive, and specific assessment of diaphragm effort. SMdi coupled with functional respiratory investigations may help to detect diaphragm dysfunction (25). Although feasibility of diaphragm SWE in the left zone of apposition (and other approaches) remain to be investigated, it might be particularly useful for detecting diaphragm hemi-paralysis. Diaphragm SWE might also be particularly relevant within spontaneous breathing trials and/or pressure support ventilation in ventilated patients during the weaning phase (22, 25). Diaphragm stiffening-time index may also be computed during spontaneous breathing trial similarly to the diaphragm excursion-time index recently proposed by Palkar et al. (24). Hence the feasibility and the performance of SMdi measurements in critically ill patients shall be assessed in future studies. Pediatric use of diaphragm SWE also remain to be addressed. The current offline setting of the data analysis impedes the use of diaphragm SWE at the bedside. Built-in mode must be developed within ultrasound scanners to allow on-site SMdi measurements. The development of a device specifically designed for this purpose may also help to apply and disseminate the use of diaphragm SWE.

In conclusion, diaphragm SWE may be used as a noninvasive and specific method for detecting stepwise increases in diaphragm effort during submaximal isovolumetric inspiratory efforts and during ventilation against inspiratory threshold loading. SMdi was strongly correlated to Pdi within both models. Further research and technological developments are required to optimize diaphragm SWE and its conditions of use for the diagnosis and follow up of diaphragm dysfunction as well as its potential for predicting weaning outcome in the ventilated patient.

Acknowledgments

We gratefully thank all the volunteers who participated in this study. This study was supported by the Association pour le Développement et l'Organisation de la Recherche en Pneumologie et sur le Sommeil (ADOREPS), the program Investissement d'Avenir ANR-10-AIHU 06 of the French Government, and the Association Française Contre Les Myopathies (AFM).

Conflict of Interest

JLG is a scientific consultant for Supersonic Imagine, Aix-en-Provence, France. MD received personal fees from Lungpacer Medical Inc., Vancouver, Canada. A request for a patent that encompasses findings presented in the present work has been filled.

References

1. **American Thoracic Society/European Respiratory S**. ATS/ERS Statement on respiratory muscle testing. *American Journal of Respiratory and Critical Care Medicine* 166: 518-624, 2002.

2. **Ates F, Hug F, Bouillard K, Jubeau M, Frappart T, Couade M, Bercoff J, and Nordez A**. Muscle shear elastic modulus is linearly related to muscle torque over the entire range of isometric contraction intensity. *Journal of Electromyography and Kinesiology* 25: 703-708, 2015.

3. **Bakdash JZ, and Marusich LR**. Repeated Measures Correlation. *Front Psychol* 8: 456, 2017.

4. **Bercoff J, Tanter M, and Fink M**. Supersonic shear imaging: a new technique for soft tissue elasticity mapping. *IEEE Transactions on Ultrasonics Ferroelectrics and Frequency Control* 51: 396-409, 2004.

5. **Chen R, Kayser B, Yan S, and Macklem PT**. Twitch transdiaphragmatic pressure depends critically on thoracoabdominal configuration. *J Appl Physiol (1985)* 88: 54-60, 2000.

6. **Chen RC, Que CL, and Yan S**. Introduction to a new inspiratory threshold loading device. *Eur Respir J* 12: 208-211, 1998.

7. **Chino K, Ohya T, Katayama K, and Suzuki Y**. Diaphragmatic shear modulus at various submaximal inspiratory mouth pressure levels. *Respir Physiol Neurobiol* 252-253: 52-57, 2018.

8. **Couade M, Pernot M, Messas E, Bel A, Ba M, Hagege A, Fink M, and Tanter M**. In vivo quantitative mapping of myocardial stiffening and transmural anisotropy during the cardiac cycle. *IEEE Transactions on Medical Imaging* 30: 295-305, 2011.

9. **Doorduin J, Sinderby CA, Beck J, Stegeman DF, van Hees HW, van der Hoeven JG, and Heunks LM**. The calcium sensitizer levosimendan improves human diaphragm function. *American Journal of Respiratory and Critical Care Medicine* 185: 90-95, 2012.

10. **Dres M, Goligher EC, Dube BP, Morawiec E, Dangers L, Reuter D, Mayaux J, Similowski T, and Demoule A**. Diaphragm function and weaning from mechanical ventilation: an ultrasound and phrenic nerve stimulation clinical study. *Ann Intensive Care* 8: 53, 2018.

11. **Dube BP, and Dres M**. Diaphragm Dysfunction: Diagnostic Approaches and Management Strategies. *Journal of Clinical Medicine* 5: 113, 2016.

12. **Dube BP, Dres M, Mayaux J, Demiri S, Similowski T, and Demoule A**. Ultrasound evaluation of diaphragm function in mechanically ventilated patients: comparison to phrenic stimulation and prognostic implications. *Thorax* 72: 811-818, 2017.

13. **Ewertsen C, Carlsen JF, Christiansen IR, Jensen JA, and Nielsen MB**. Evaluation of healthy muscle tissue by strain and shear wave elastography - Dependency on depth and ROI position in relation to underlying bone. *Ultrasonics* 71: 127-133, 2016.

14. **Gandevia SC, McKenzie DK, and Plassman BL**. Activation of human respiratory muscles during different voluntary manoeuvres. *J Physiol* 428: 387-403, 1990.

15. **Gennisson JL, Cornu C, Catheline S, Fink M, and Portero P**. Human muscle hardness assessment during incremental isometric contraction using transient elastography. *Journal of Biomechanics* 38: 1543-1550, 2005.

16. **Gennisson JL, Deffieux T, Fink M, and Tanter M**. Ultrasound elastography: principles and techniques. *Diagn Interv Imaging* 94: 487-495, 2013.

17. **Gennisson JL, Deffieux T, Mace E, Montaldo G, Fink M, and Tanter M**. Viscoelastic and anisotropic mechanical properties of in vivo muscle tissue assessed by supersonic shear imaging. *Ultrasound in Medicine and Biology* 36: 789-801, 2010.

18. **Hug F, Tucker K, Gennisson JL, Tanter M, and Nordez A**. Elastography for Muscle Biomechanics: Toward the Estimation of Individual Muscle Force. *Exercise and Sport Sciences Reviews* 43: 125-133, 2015.

19. **Koulouris N, Mulvey DA, Laroche CM, Goldstone J, Moxham J, and Green M**. The effect of posture and abdominal binding on respiratory pressures. *Eur Respir J* 2: 961-965, 1989.

20. **Laghi F, and Tobin MJ**. Disorders of the respiratory muscles. *American Journal of Respiratory and Critical Care Medicine* 168: 10-48, 2003.

21. **Lapole T, Tindel J, Galy R, and Nordez A**. Contracting biceps brachii elastic properties can be reliably characterized using supersonic shear imaging. *European Journal of Applied Physiology* 115: 497-505, 2015.

22. **Magalhaes PAF, Camillo CA, Langer D, Andrade LB, Duarte M, and Gosselink R**. Weaning failure and respiratory muscle function: What has been done and what can be improved? *Respiratory Medicine* 134: 54-61, 2018.

23. **Oppersma E, Hatam N, Doorduin J, van der Hoeven JG, Marx G, Goetzenich A, Fritsch S, Heunks LMA, and Bruells CS**. Functional assessment of the diaphragm by speckle tracking ultrasound during inspiratory loading. *J Appl Physiol (1985)* 123: 1063-1070, 2017.

24. **Palkar A, Narasimhan M, Greenberg H, Singh K, Koenig S, Mayo P, and Gottesman E**. Diaphragm Excursion-Time Index: A New Parameter Using Ultrasonography to Predict Extubation Outcome. *Chest* 153: 1213-1220, 2018.

25. **Pirompanich P, and Romsaiyut S**. Use of diaphragm thickening fraction combined with rapid shallow breathing index for predicting success of weaning from mechanical ventilator in medical patients. *J Intensive Care* 6: 6, 2018.

26. **Sarwal A, Walker FO, and Cartwright MS**. Neuromuscular ultrasound for evaluation of the diaphragm. *Muscle & Nerve* 47: 319-329, 2013.

27. **Similowski T, Duguet A, Straus C, Attali V, Boisteanu D, and Derenne JP**. Assessment of the voluntary activation of the diaphragm using cervical and cortical magnetic stimulation. *Eur Respir J* 9: 1224-1231, 1996.

352 28. **Team RC**. R: A Language and Environment for Statistical Computing. 2017.

353 29. **Umbrello M, Formenti P, Longhi D, Galimberti A, Piva I, Pezzi A, Mistraletti G, Marini JJ, and**
354 **Iapichino G**. Diaphragm ultrasound as indicator of respiratory effort in critically ill patients undergoing
355 assisted mechanical ventilation: a pilot clinical study. *Critical Care* 19: 161, 2015.

356 30. **Verges S, Bachasson D, and Wuyam B**. Effect of acute hypoxia on respiratory muscle fatigue in
357 healthy humans. *Respiratory Research* 11: 109, 2010.

358 31. **Zambon M, Greco M, Bocchino S, Cabrini L, Beccaria PF, and Zangrillo A**. Assessment of
359 diaphragmatic dysfunction in the critically ill patient with ultrasound: a systematic review. *Intensive Care*
360 *Medicine* 43: 29-38, 2017.

361

Tables

Table 1. Pressures and diaphragm shear modulus during apnea and during isovolumetric inspiratory efforts against closed airways.

	target (%PImax)						
variables	**0**	**10**	**20**	**30**	**40**	**50**	**60**
mean Pmo (% PImax)	-	10.2 (1.6)	19.0 (1.9)*	29.1 (2.5)*	39.1 (3.2)*	47.7 (3.0)*	56.5 (4.8)*
mean Pes (cmH_20)	3.8 (2.9)	-8.8 (5.3)	-16.7 (9.0)*	-26.8 (12.4)*	-37.1 (16.3)*	-45.6 (20.7)*	-55.8 (19.4)*
mean Pga (cmH_20)	10.9 (2.9)	16.9 (9.5)*	14.7 (3.8)*	16.2 (5.4)*	15.6 (5.1)*	17.6 (6.6)*	17.0 (9.8)*
mean Pdi (cmH_20)	14.8 (3.5)	25.8 (11.1)*	31.4 (10.3)*	43.0 (12.6)*	52.7 (16.7)*	63.1 (20.7)*	72.9 (24.8)*
mean SMdi (kPa)	0.6 (0.6)	7.3 (6.0)*	9.0 (6.5)*	15.2 (9.7)*	18.7 (9.9)*	25.9 (9.7)*	28.9 (12.6)*

Data are shown as mean (SD). Data from two trials for each condition were averaged. Target (% PImax), targeted pressure expressed as a percentage of maximal voluntary isovolumetric inspiratory pressure with 0% PImax corresponding to measurements during apnea at functional residual capacity ; mean Pmo (% PImax), mean mouth pressure expressed as a percentage of PImax; Pes, esophageal pressure; Pga, gastric pressure; Pdi, transdiaphragmatic pressure, SMdi, diaphragm shear modulus.*significantly different from 0% PImax ($p < 0.05$).

371 **Table 2.** Relationship between diaphragm shear modulus during isovolumetric inspiratory efforts against closed
372 airways in all participants.

Participants	*r* [95% CI]	*p* value
1	0.79 [0.39-0.94]	< 0.01
2	0.87 [0.64-0.96]	< 0.001
3	0.92 [0.77-0.98]	< 0.001
4	0.91 [0.73-0.97]	< 0.001
5	0.92 [0.76-0.97]	< 0.001
6	0.92 [0.76-0.97]	< 0.001
7	0.86 [0.60-0.95]	< 0.001
8	0.95 [0.84-0.98]	< 0.001
9	0.88 [0.67-0.96]	< 0.001
10	0.77 [0.31-0.94]	< 0.01
11	0.96 [0.88-0.99]	< 0.001
12	0.80 [0.47-0.93]	< 0.001
13	0.85 [0.58-0.95]	< 0.001

373 r [95% CI], Pearson correlation coefficient with lower and higher 95% confidence intervals.

Table 3. Flow, pressures, and diaphragm shear modulus during unloaded ventilation and ventilation against inspiratory threshold loading.

	threshold loading (% PImax)					
variables	**0**	**10**	**20**	**30**	**40**	**50**
Bf (breaths/min)	12.0 (2.2)	13.3 (2.8)	12.3 (2.8)	12.9 (3.1)	12.3 (3.0)	12.9 (4.2)
EE Pes (cmH_20)	4.3 (2.8)	2.8 (2.0)	2.4 (2.6)	4.1 (1.8)	6.3 (4.0)	7.1 (3.7)*
VT (l)	0.5 (0.7)	0.8 (0.7)	0.8 (0.8)	0.6 (0.7)	0.6 (0.8)	0.5 (0.7)
TI (s)	2.1 (0.3)	2.5 (0.5)	2.8 (0.6)	2.8 (0.6)	2.9 (0.8)	3.0 (1.0)
VT/TI	0.2 (0.3)	0.4 (0.4)	0.3 (0.3)	0.2 (0.3)	0.2 (0.3)	0.2 (0.3)
TI/TT	0.4 (0.0)	0.5 (0.1)	0.6 (0.1)	0.6 (0.1)	0.6 (0.1)	0.6 (0.1)
mean Pch (cmH_20)	4.1 (1.3)	-12.9 (2.7)*	-24.4 (5.8)*	-36.4 (9.2)*	-48.2 (10.8)*	-59.2 (14.4)*
Δ Pmo (% PImax)	1.7 (0.5)	19.6 (2.6)*	29.6 (3.6)*	39.0 (4.5)*	46.6 (6.6)*	54.2 (9.3)*
Δ Pes (cmH_20)	-8.5 (2.6)	-27.2 (9.9)	-38.4 (14.6)*	-48.2 (16.1)*	-60.4 (18.9)*	-67.8 (21.5)*
Δ Pga (cmH_20)	6.3 (2.2)	7.6 (5.2)	9.9 (6.1)*	10.1 (4.7)*	8.8 (2.6)*	8.7 (2.2)*
Δ Pdi (cmH_20)	10.4 (4.4)	29.8 (13.8)*	42.3 (18.3)*	49.4 (17.9)*	59.1 (20.9)*	63.6 (23.1)*
max SMdi (kPa)	6.2 (3.6)	16.0 (8.5)*	24.3 (10.0)*	27.8 (13.8)*	32.5 (13.8)*	35.7 (13.4)*

Data are shown as mean (SD). Data from each cycle for a given loading level were averaged. Threshold loading (% PImax), inspiratory threshold loading expressed as a percentage of maximal voluntary isovolumetric inspiratory pressure with 0% PImax corresponding to unloaded ventilation; Bf, breathing frequency; EE Pes, end-expiratory esophageal pressure; VT, tidal volume; TI, inspiratory time; VT /TI, tidal volume to inspiratory time ratio *i.e* inspiratory flow; TI/TT, ratio of inspiratory to total time of the respiratory cycle *i.e.* duty cycle; mean Pch, mean chamber pressure within the inspiratory loading device. Pmo, variation of mouth pressure during inspiratory time; Δ Pmo, variation of mouth pressure during inspiratory time; Δ Pes, variation of esophageal pressure during inspiratory time; Δ Pga, variation of gastric pressure during inspiratory time; Δ Pdi, variation of transdiaphragmatic pressure during inspiratory time; max SMdi, maximal diaphragm shear modulus

during the inspiratory time. TFdi, diaphragm thickening fraction. *significantly different from unloaded breathing *i.e.* threshold loading 0 % PImax (p <0.05).

Table 4. Relationship between diaphragm shear modulus during unloaded ventilation and ventilation against inspiratory threshold loading in all participants.

Participants	***r* [95% CI]**	***p* value**
1	0.73 [0.59-0.83]	< 0.001
2	0.85 [0.76-0.90]	< 0.001
3	0.90 [0.84-0.94]	< 0.001
4	0.90 [0.84-0.94]	< 0.001
5	0.40 [0.18-0.59]	< 0.001
6	0.79 [0.68-0.86]	< 0.001
7	0.86 [0.77-0.91]	< 0.001
8	0.87 [0.80-0.92]	< 0.001
10	0.55 [0.21-0.78]	< 0.01
12	0.44 [0.22-0.61]	< 0.001
13	0.67 [0.47-0.80]	< 0.001
14	0.82 [0.73-0.89]	< 0.001
15	0.76 [0.64-0.85]	< 0.001

r [95% CI], Pearson correlation coefficient with lower and higher 95% confidence intervals.

Figures

Figure 1. Overview of the experimental setup.

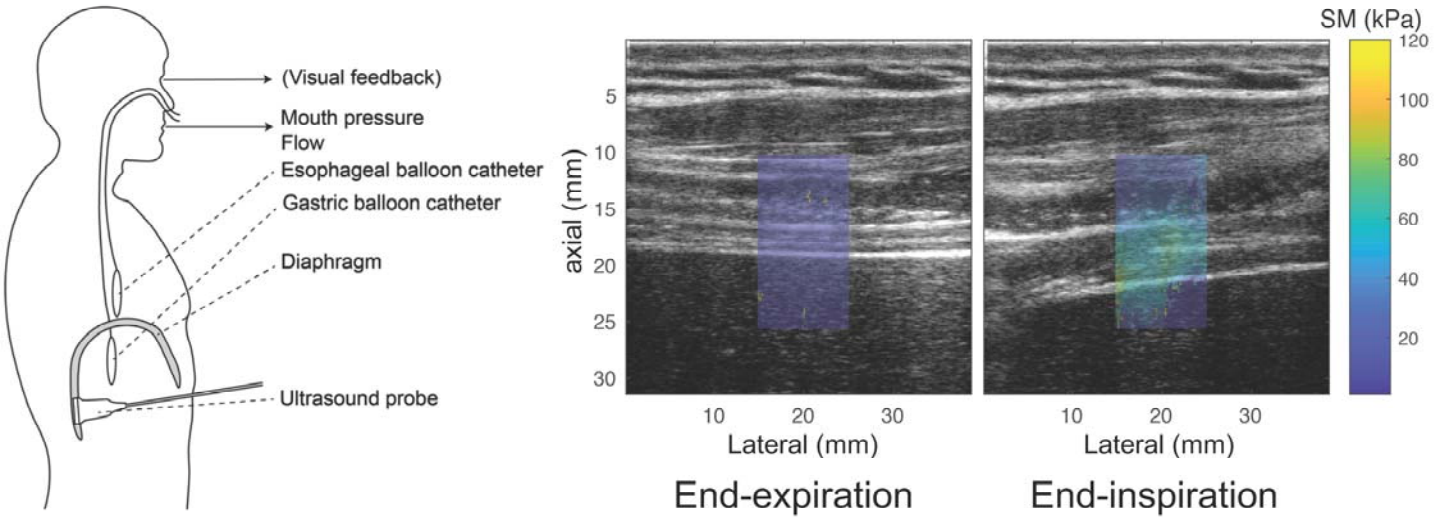

The left panel shows the experimental setup with respiratory measurements and intercostal diaphragm ultrasound imaging. Visual feedback of generated mouth pressure and guidelines were provided during isovolumetric inspiratory efforts against closed airways. The right panel shows the shear modulus (SM) map in kPa measured using shear wave elastography overlaid with standard B-Mode at end-expiration and end-inspiration during ventilation against inspiratory threshold loading.

Figure 2. Typical measurements during isovolumetric inspiratory efforts against closed airways in participant #3.

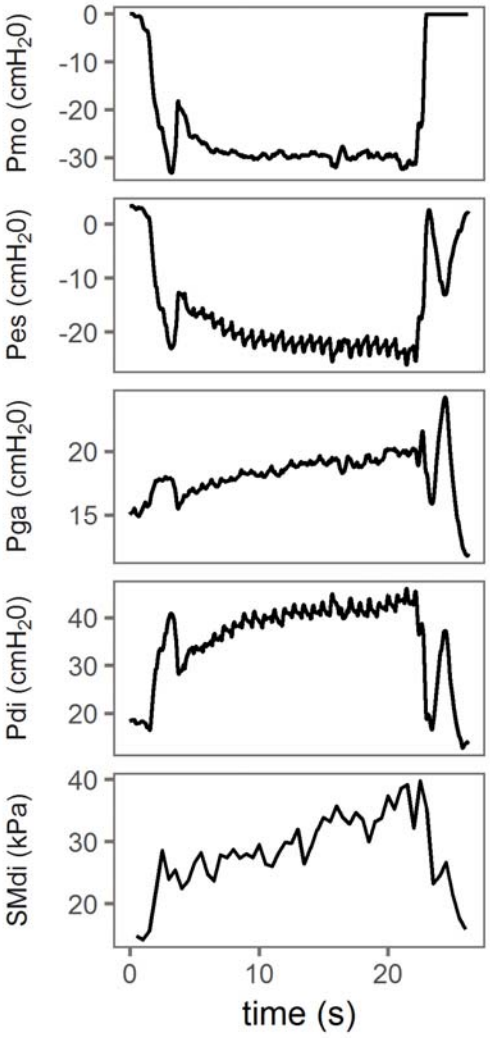

Pmo, mouth pressure; Pes, esophageal pressure; Pga, gastric pressure; Pdi, transdiaphragmatic pressure, SMdi, diaphragm shear modulus.

Figure 3. Relationship between transdiaphragmatic pressure and diaphragm shear modulus during submaximal isovolumetric inspiratory efforts against closed airways (n=13).

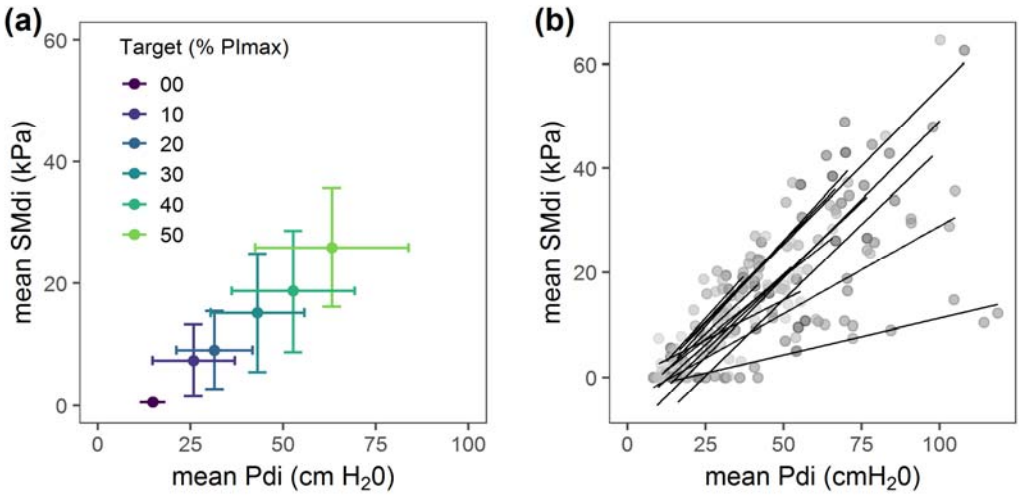

Panel (a): average values per condition i.e. apnea at functional residual capacity and submaximal isovolumetric inspiratory efforts at 10, 20, 30, 40, 50 % of maximal inspiratory pressure (PI max). Panel (b): all data points with individual linear regression lines; mean SMdi, mean diaphragm shear modulus; mean Pdi, mean transdiaphragmatic pressure.

Figure 4. Individual data points illustrating relationship between transdiaphragmatic pressure and diaphragm shear modulus during submaximal isovolumetric inspiratory efforts against closed airways.

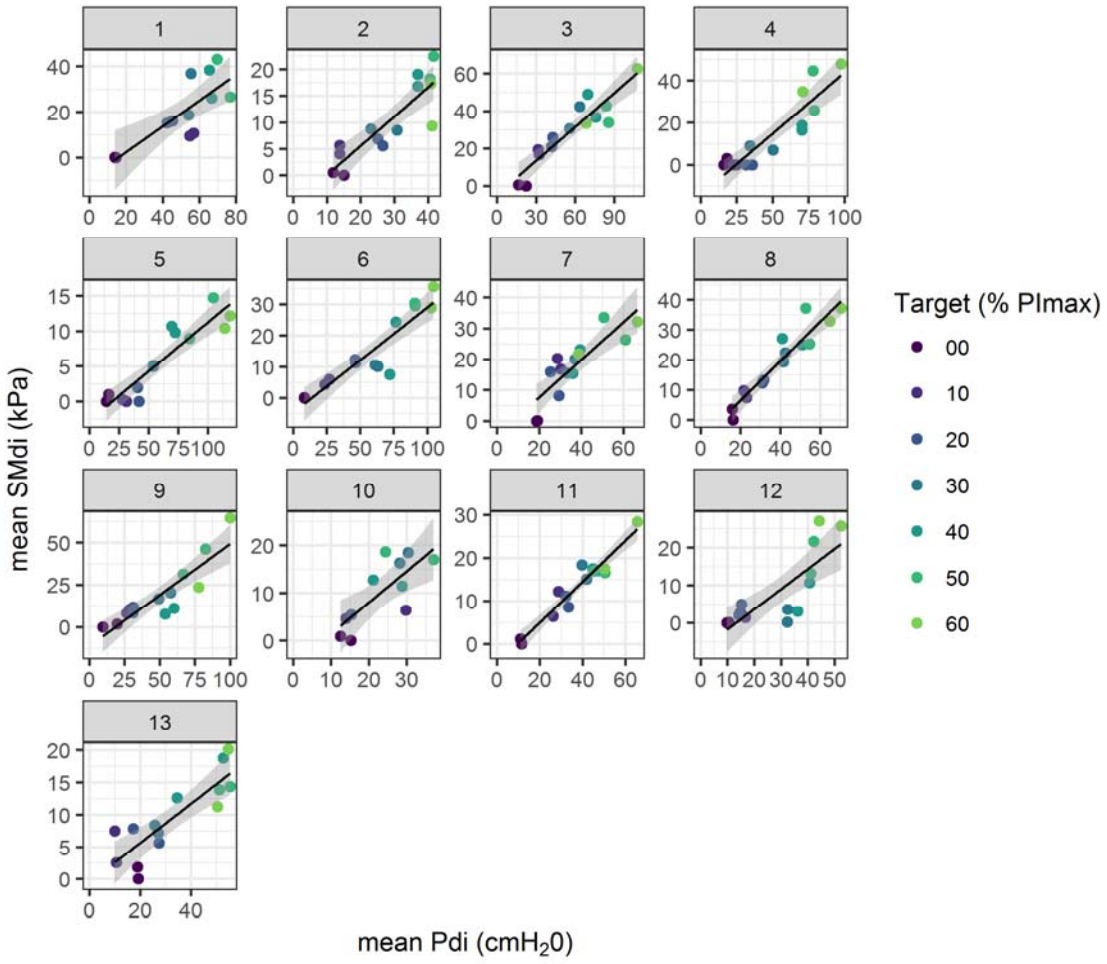

Figure 5. Typical measurements during ventilation against inspiratory threshold loading in participant #1.

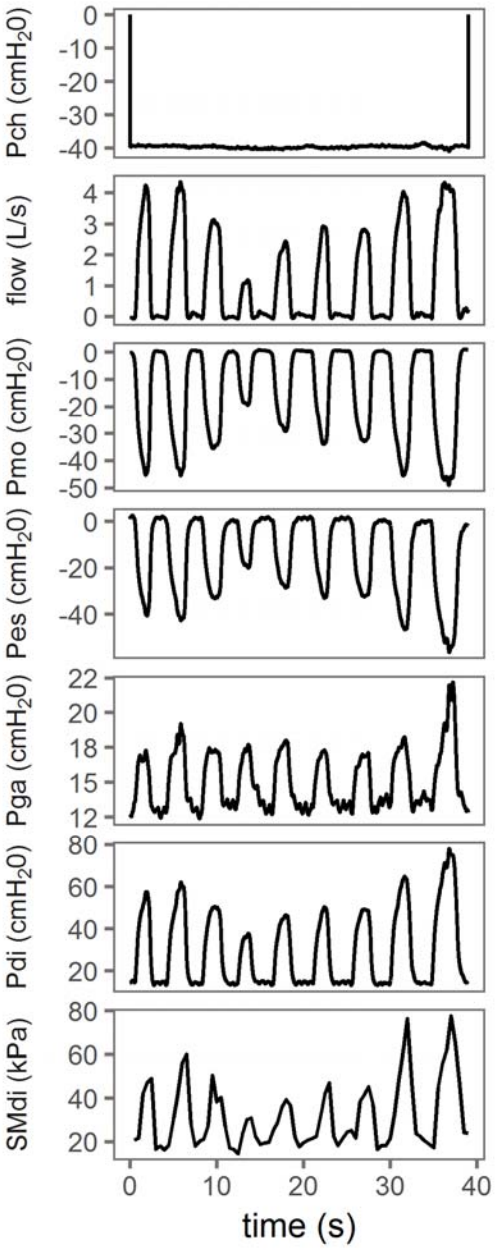

Pch, chamber pressure with the inspiratory threshold loading device; Pmo, mouth pressure; Pes, esophageal pressure; Pga, gastric pressure; Pdi, transdiaphragmatic pressure, SMdi, diaphragm shear modulus.

Figure 6. Relationship between transdiaphragmatic pressure and diaphragm shear modulus during unloaded ventilation and ventilation against inspiratory threshold loading (n=15).

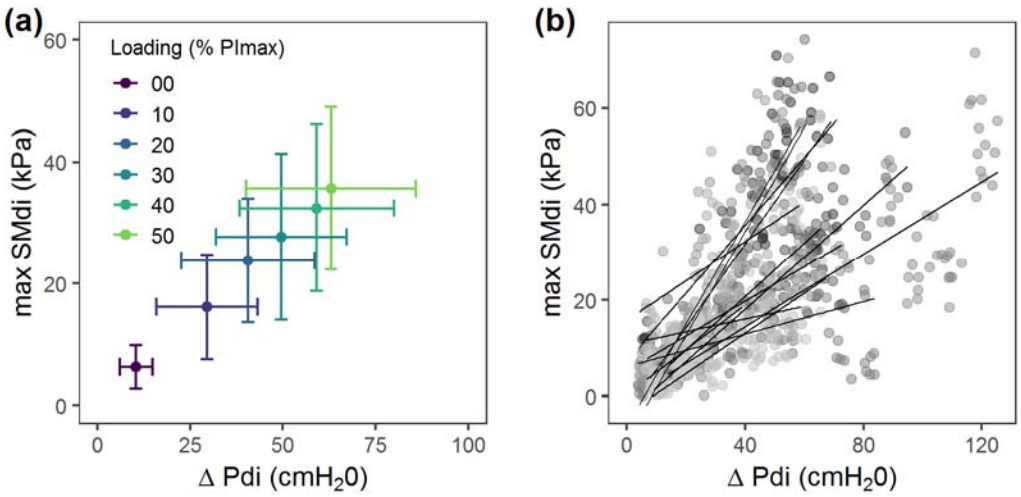

Panel (a): average values per condition i.e. spontaneous ventilation capacity and ventilation against inspiratory threshold loading at 10, 20, 30, 40, 50 % of maximal inspiratory pressure (PI max). Panel (b): all data points with individual linear regression lines. max SMdi, maximal diaphragm shear modulus during the inspiratory time; Δ Pdi, variation (swing) of transdiaphragmatic pressure during the inspiratory time.

Figure 7. Individual data points illustrating relationship between transdiaphragmatic pressure and diaphragm shear modulus during unloaded ventilation and ventilation against inspiratory threshold loading.

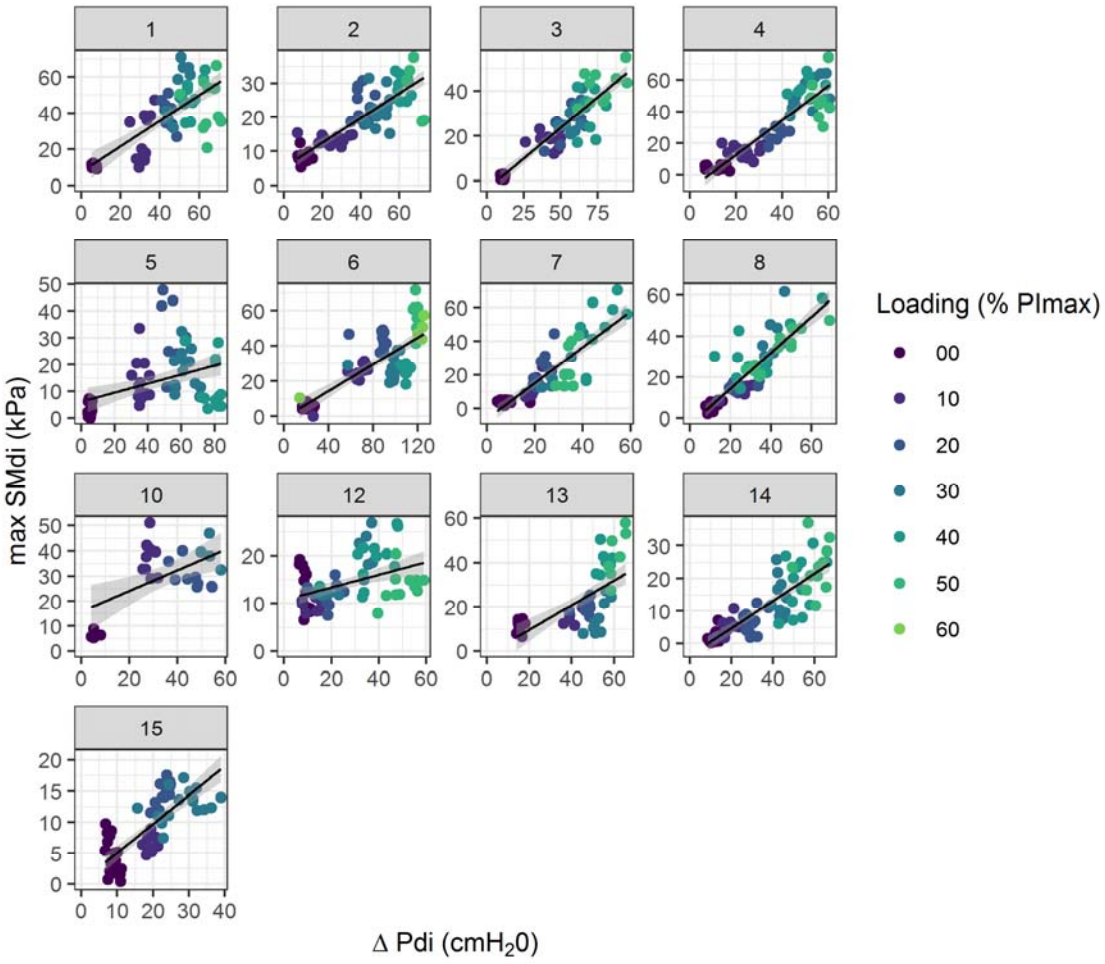

max SMdi, maximal diaphragm shear modulus during the inspiratory time; Δ Pdi, variation (swing) of transdiaphragmatic pressure during the inspiratory time; loading (% PImax), inspiratory threshold loading expressed as a percentage of maximal inspiratory pressure.

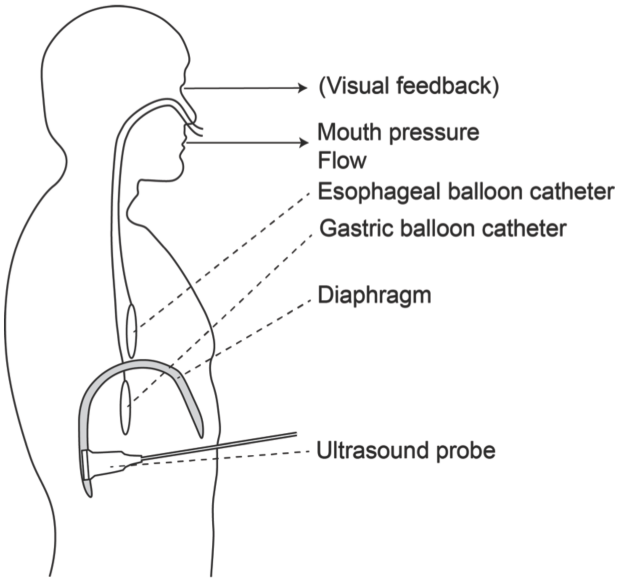
(Visual feedback)
Mouth pressure
Flow
Esophageal balloon catheter
Gastric balloon catheter
Diaphragm
Ultrasound probe

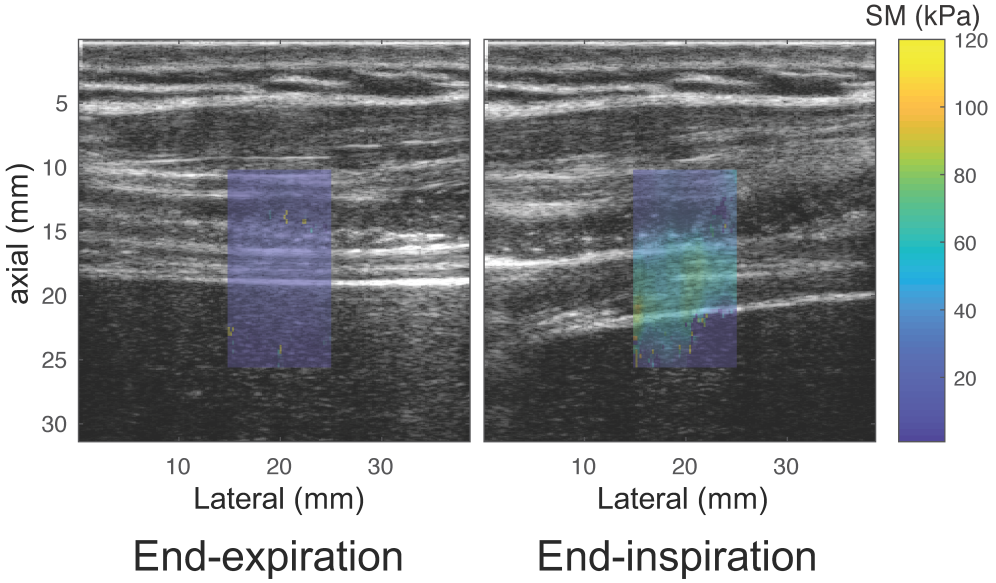
SM (kPa)
120
100
80
60
40
20
axial (mm)
5
10
15
20
25
30
10
20
30
Lateral (mm)
10
20
30
Lateral (mm)
End-expiration
End-inspiration

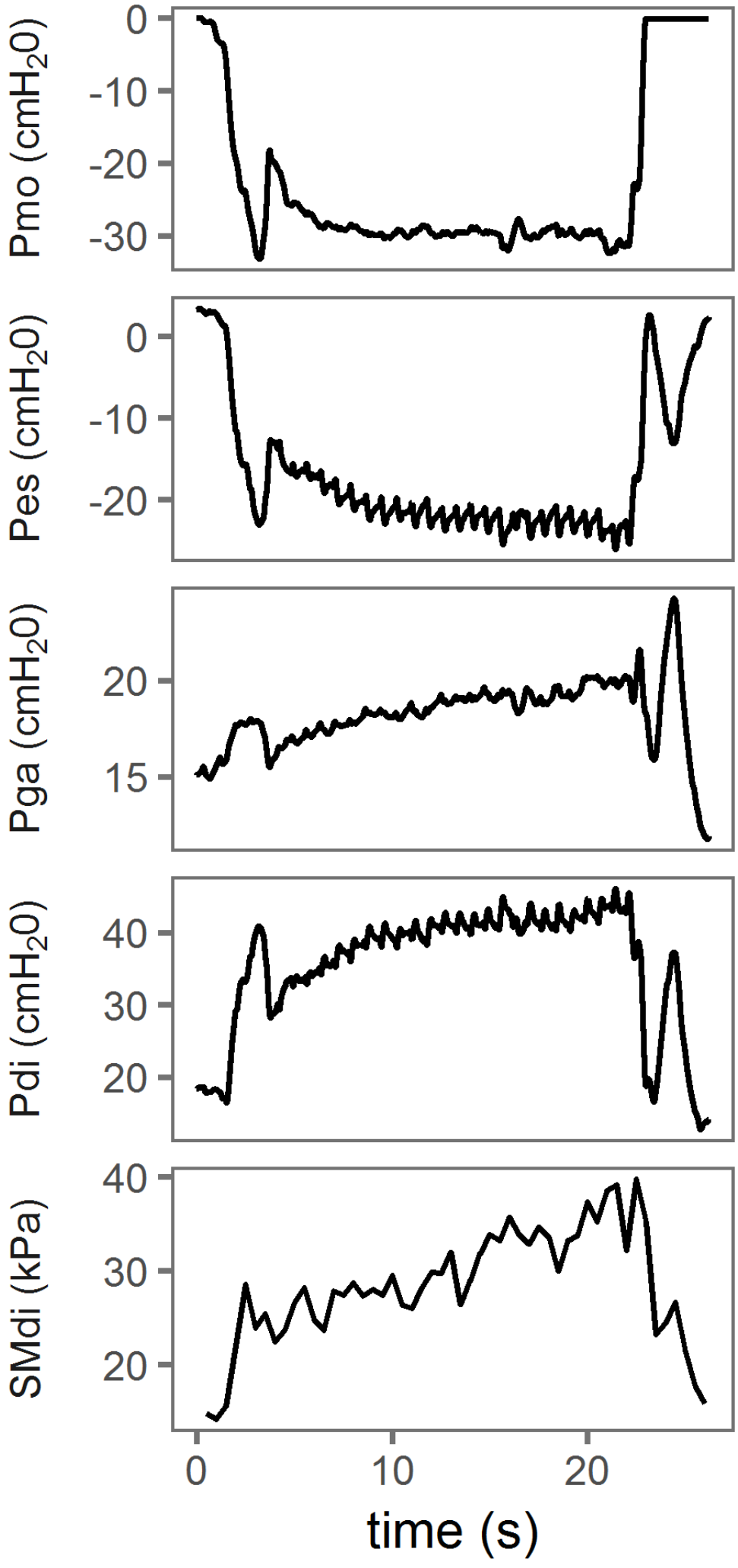
Pmo (cmH20)
0
-10
-20
-30
Pes (cmH20)
0
-10
-20
Pga (cmH20)
20
15
Pdi (cmH20)
40
30
20
SMdi (kPa)
40
30
20
0
10
20
time (s)

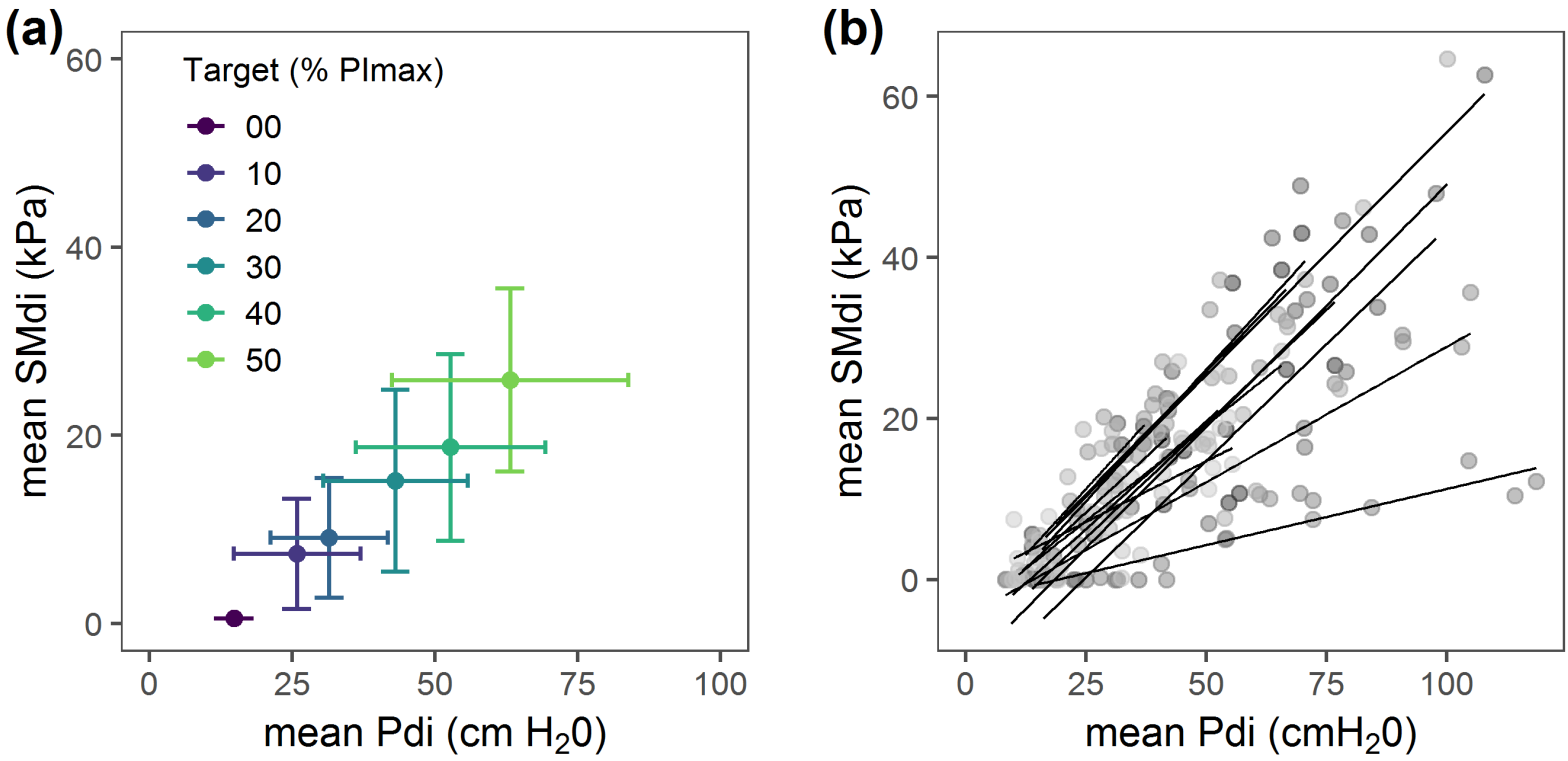
(a)
Target (% PImax)
00
10
20
30
40
50
mean SMdi (kPa)
mean Pdi (cm H20)
0
20
40
60
0
25
50
75
100
(b)
mean SMdi (kPa)
mean Pdi (cmH20)
0
20
40
60
0
25
50
75
100

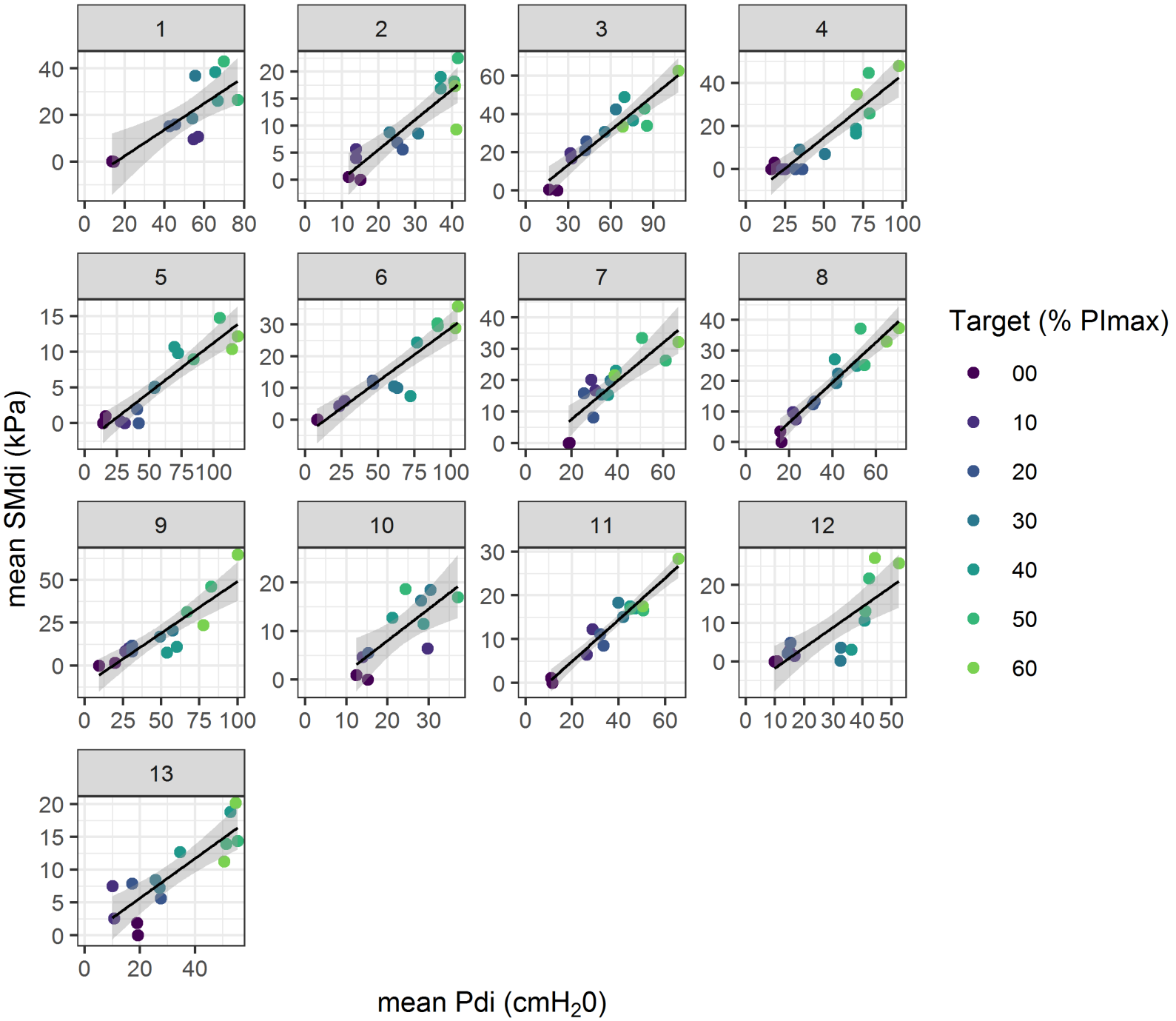
1
2
3
4
5
6
7
8
9
10
11
12
13
mean SMdi (kPa)
mean Pdi (cmH20)
Target (% PImax)
00
10
20
30
40
50
60

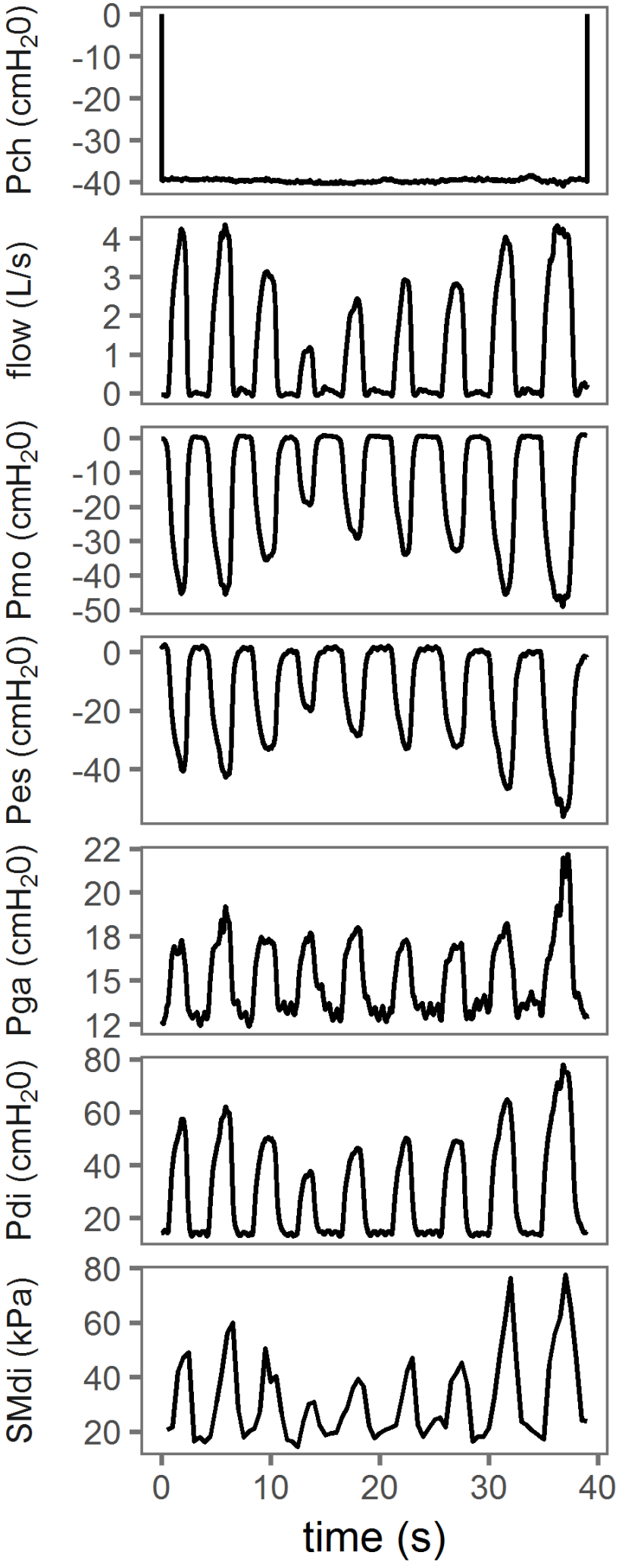
Pch (cmH20)
0
-10
-20
-30
-40
flow (L/s)
4
3
2
1
0
Pmo (cmH20)
0
-10
-20
-30
-40
-50
Pes (cmH20)
0
-20
-40
Pga (cmH20)
22
20
18
15
12
Pdi (cmH20)
80
60
40
20
SMdi (kPa)
80
60
40
20
0
10
20
30
40
time (s)

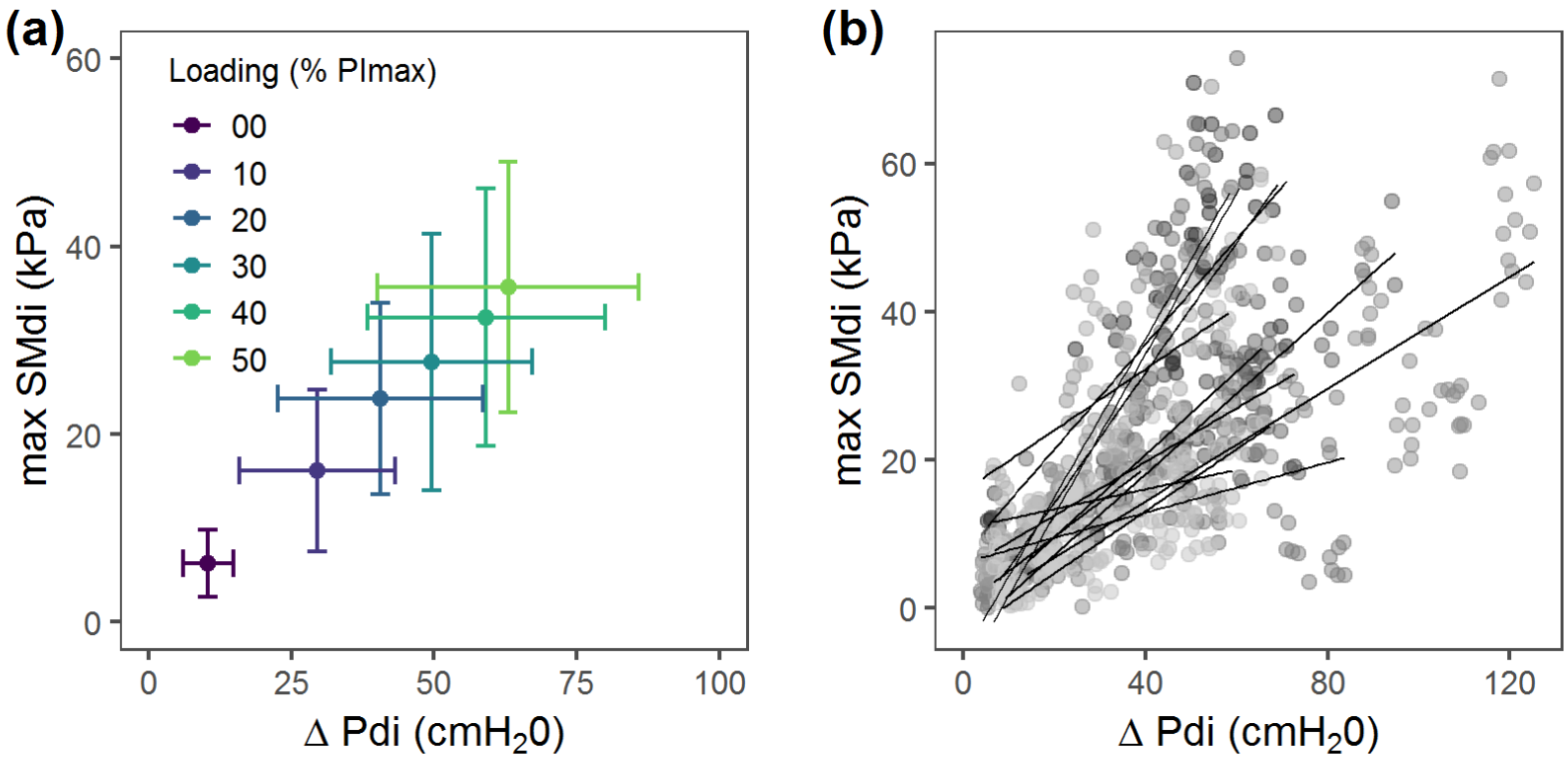
(a)
Loading (% PImax)
00
10
20
30
40
50
max SMdi (kPa)
0
20
40
60
0
25
50
75
100
Δ Pdi (cmH20)
(b)
max SMdi (kPa)
0
20
40
60
0
40
80
120
Δ Pdi (cmH20)

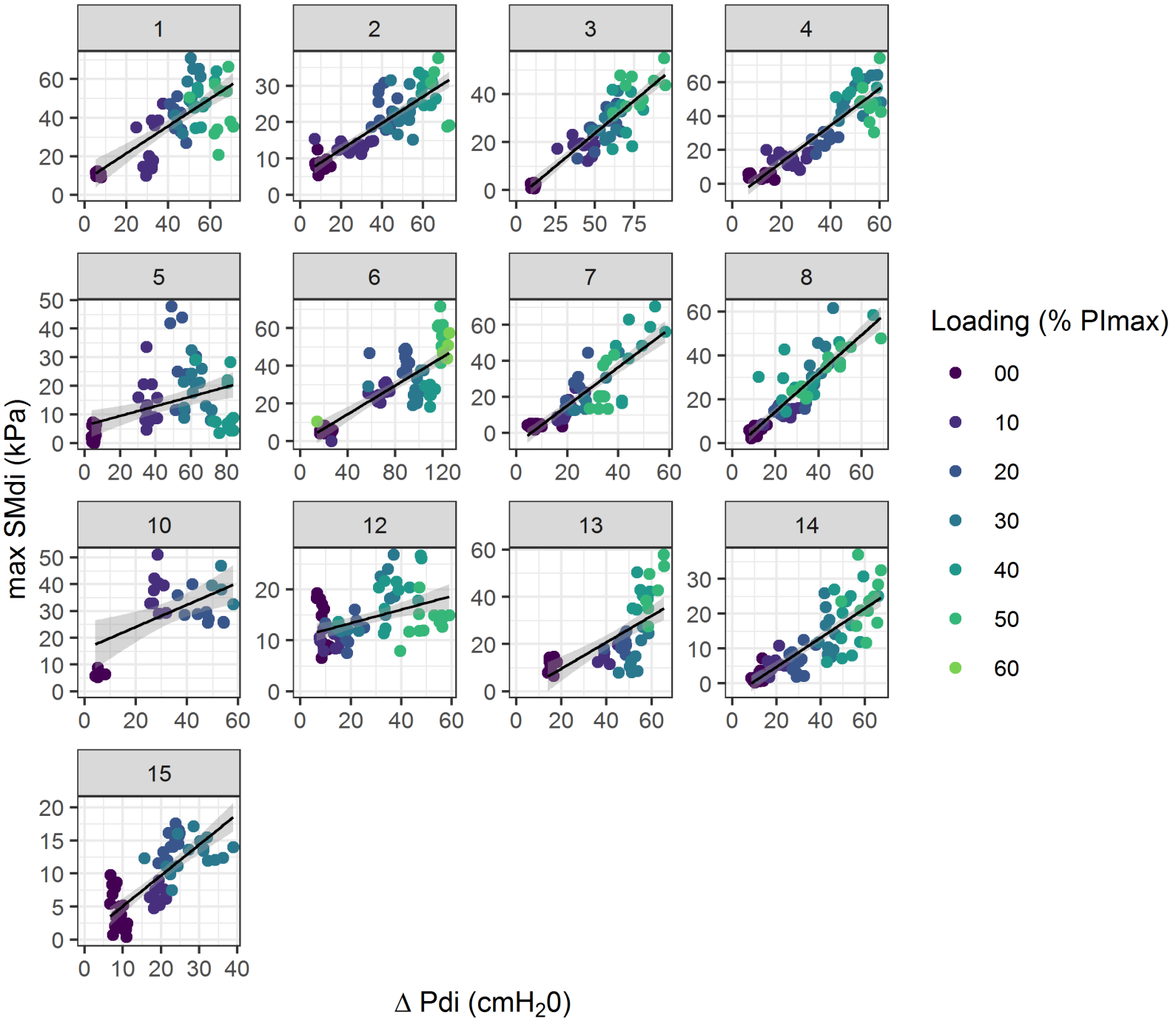
1
2
3
4
5
6
7
8
10
12
13
14
15
max SMdi (kPa)
Δ Pdi (cmH20)
Loading (% PImax)
00
10
20
30
40
50
60